4.1 Introduction

So far, we have analyzed the basic configuration of the ARROW waveguide that will be used for obtaining integrated optical devices. The processes that allow obtaining not only ARROW structures, but any device based on these waveguides has also been studied. Although some indications have already been given, this chapter is focused on the problems that nowadays some structures have, and some proposals for solving them or new configurations are presented. Moreover, the devices highlighted in chapter 2 have been designed and simulated. Design has been done according to the fabrication limitations above presented, and simulations will be shown straightforward. Concrete fabrication steps and experimental results will be seen at the beginning of the next chapter.

For clarification, from now on integrated optical devices will be separately treated and explained. This asset will help us giving more emphasis on the variables that affect a given device, paying low attention to the irrelevant ones. Logically, the first device that has to be studied, although the term *device* is ambiguous in this case, is the waveguide itself. In chapter 2, it was seen some of their optical properties, both analytically and on numerical simulations. Now, some additional aspects will be studied.

4.2 Waveguides

In chapter 2 it was seen that ARROW waveguides where monomode in the z direction, but that depending on the rib height, several lateral modes, that could be labeled as TE_{0x} (x = 0,1...) were able to propagate through the waveguide with losses having similar order of magnitude. It has been seen that some applications require a monomode behavior in the cross section, that is, only having the TE_{00} mode. This behavior can be achieved by decreasing the rib height (for wide waveguides) or making waveguides narrower (for high ribs). However, in both cases a decrease of the confinement factor on the structure is observed. It has previously discussed that the cross-section confinement is due to rib etch, that causes the effective refractive index of the non-etched zone to be higher as compared to the surroundings, obtaining what could be called an effective TIR structure. The single mode waveguide shown in fig 4.1a, with given width and rib, is provided as a reference. For a fixed width, if the rib depth decreases, as observed in fig. 4.1b, the effective index values between the core and the surrounding layers are closer, causing the lateral evanescent tail to be enhanced, being the mode less confined on the structure. If waveguides are made narrower for a fixed rib (figure 4.1c). Core dimensions of the effective structure in the *y* axis is also reduced, causing the mode to be closer to cutoff conditions in the y direction and being poorly confined within the waveguide. Moreover, as far as technological steps are concerned, deep etching requires a hard photoresist pre-baking that, depending on the precursors gases employed, is suitable to cause polymerization on the wafer surface that will prevent from further etch.

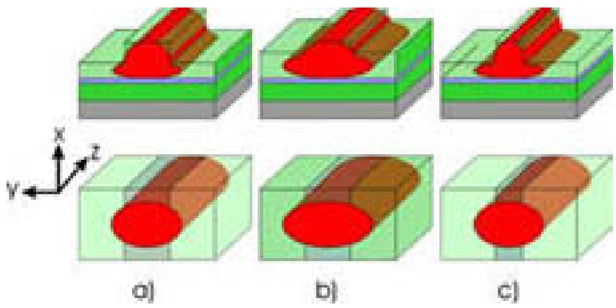

Fig 4.1. ARROW waveguides and its effective structures, where it can be seen that both a decrease of the width or a minor rib causes the field to be less confined.

In most integrated optic devices, high confinement is essential if changes in the light path want to be done, as could be Y-junctions or bendings. As a rule, for ARROW waveguides with a core of 4µm, rib etch smaller than 1µm or width below 4µm present monomode behavior but with low confinement. Rib that assures good confinement should be at least 50% of the core thickness. Previously presented experimental results with 65% etching **[1]** have proved that waveguides wider than 7µm have multimode behavior.

Thus, the rib causes the guiding structure to act laterally as a standard waveguide with effective refractive index values. Its lateral modal properties are still restricted to the conditions imposed by TIR guiding. One possibility that could overcome this problem would be also having ARROW behavior in the lateral direction.

That is, obtaining what has been labeled as ARROW-2D structures. Its basic configurations can be seen in figure 4.2.

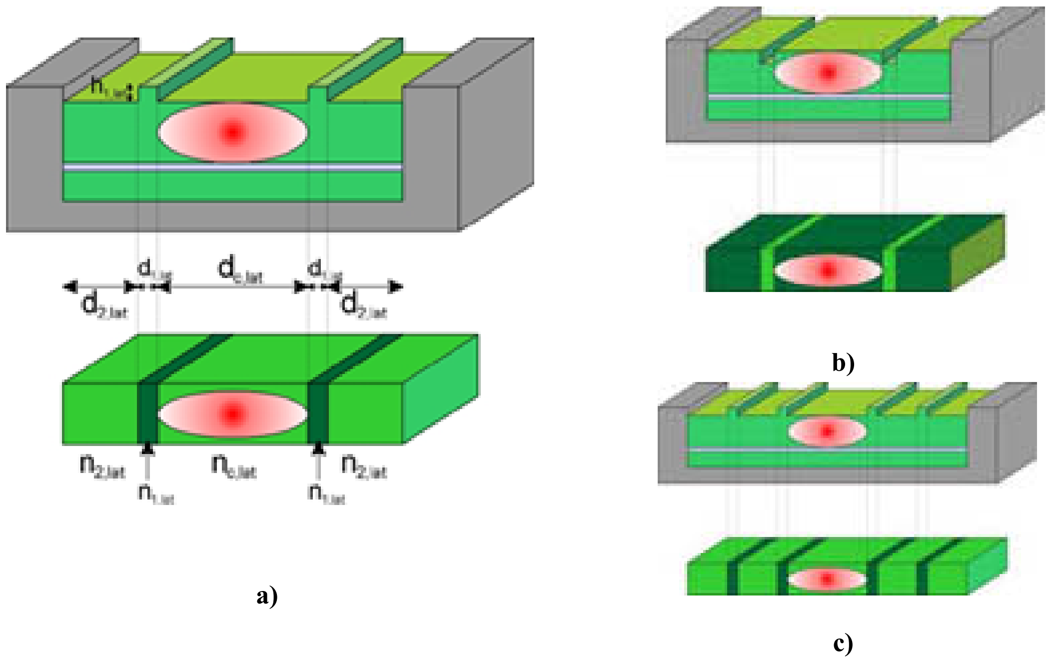

Fig 4.2. ARROW-2D structures proposed, in ARROW-A (a), ARROW-B (b) and ARROW-A with double pair antiresonant (c).

It basically consists on small weightings or trenches over the basic slab ARROW structures that causes the appropriate changes in the effective index so as to laterally behave as the first cladding of an ARROW-A (fig 4.2 a) or an ARROW-B (fig 4.2b). The second cladding in the *x* (horizontal) axis is achieved by leaving a distance $d_{2,lat}=d_{c,lat}/2$ between the lateral 1st cladding antiresonant structure (LAS) and the waveguide edges. The main advantage of this type of structure is that it is possible to place several LAS, forming multi-ARROW structures (fig. 4.2c), as opposite to rib-ARROW waveguides, where if a double antiresonant structure was deposited under the core, it could crack due to excessive mechanical stresses.

We will focus only in the two-dimensional ARROW-A structure, with single and double LAS located at both sides of the core. The main reason why choosing this structure is due to its periodical attenuation behavior, that will allow to confirm that the ARROW-2D structure works exactly in the same way as a vertical ARROW-A does. From chapter 2, we know the optimum working conditions for ARROW-A structures.

Now, however, a significant variation occurs due to the fact that we have antiresonant configuration at both sides of the core. Thus, we can focus our attention on the design of a strong lateral antiresonant pair. It was also shown that the antiresonant confinement was optimum when the refractive index difference between the core and the first cladding layer was the highest. For ARROW-2D structures what will be required is that the effective refractive index difference between these of the lateral core ($n_{c,lat}$) and the lateral 1st cladding ($n_{1,lat}$) to be the highest available. First problem arises from the fact shown in fig. 4.3. Sharp variations of the dispersion (effective refractive index) are obtained at core sizes around 2µm. However, high attenuation is obtained for core thickness below 3µm. On the contrary, for d_c values (>5µm), although low losses can be achieved, refractive index variation is so small that LAS would be excessively weak so as to confine the mode on the core. Hence, d_c will be chosen to be 3µm, reaching an agreement between the attenuation in the *y* direction and the necessary flexibility when defining the LAS in the *x*-axes.

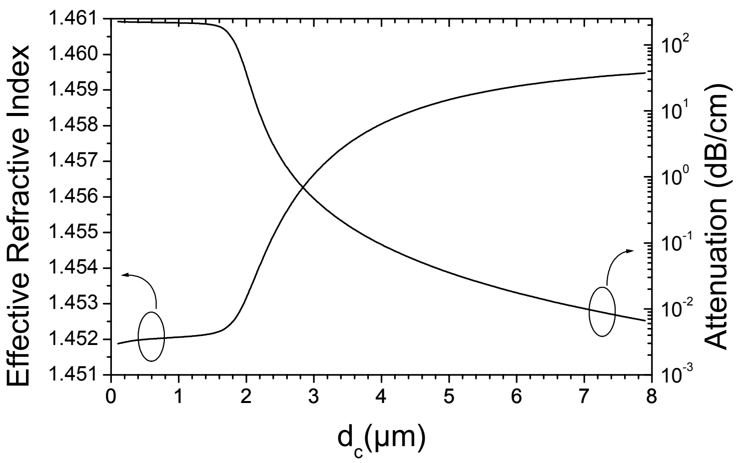

Fig 4.3. Dispersion and attenuation for the lowest order mode in an ARROW-A structure as a function of the core thickness.

The first step on analyzing these waveguides will be fixing the lateral core sizes where single mode behavior is achieved. Attenuation is presented in figure 4.4 for an ARROW-2D structure being Δn_{ce}=0.46; Δn_{c2}=0.0; d_c=3µm, d_1=0.35 and $d_{1,lat}$ (LAS width) fixed by the lateral antiresonant condition. Firstly, it can be observed how the ARROW-2D waveguide support two different kinds of modes: the ARROW modes and those propagating through the LAS (LAS modes). It has to be noted that although the main purpose of $d_{1,lat}$ is causing a local increase of the refractive index, the overall shape of the ARROW-2D structure is identical to that of a rib directional coupler. Then, LAS modes could be understood as the symmetrical and asymmetrical modes of a directional coupler that consists of two waveguides with width $d_{1,lat}$ distanced a length $d_{c,lat}$. The fact that these modes coexist with ARROW modes is not a drawback, since it has the same properties as the previously studied rib ARROW-A waveguides where, instead of the 1st cladding modes, we have directional coupler modes. The working principle and optimization of directional couplers will be deeply studied in the next subsection.

As $h_{1,lat}$ (LAS height) increases in ARROW-2D, the confinement increases due to a stronger LAS and attenuation is slightly reduced (fig. 4.4). This variation is small due to the small effective index difference caused by the variation of $h_{1,lat}$. It is also shown, as it was in chapter 2, that as the core dimensions increase, all modes progressively have lower attenuation. Thus, it is possible to define single mode cross-section waveguides with core width up to 25µm with theoretical attenuation lower than 0.4dB/cm.

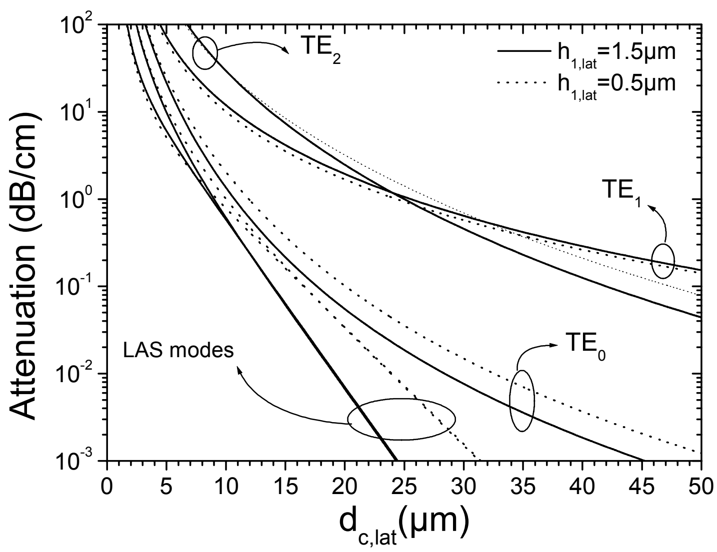

Fig 4.4. Attenuation as a function of the lateral core thickness for two different weightings. $d_{1,lat}$ has been fixed at its antiresonant value.

Attenuation and dispersion results for two different values of $h_{1,lat}$ as a function of the LAS width are shown in fig. 4.5 for the lowest order modes. Exactly in the same shape of the rib ARROW-A behavior described in chapter 2, modal transitions between the ARROW modes and the LAS modes are obtained. Differences arise from the fact that with the configuration under study, ARROW modes are not transformed to $d_{1,lat}$ modes, but to symmetrical modes ($TE_{sym,0}$) of the directional coupler formed by the two LAS (fig 4.5a). It also can be observed local attenuation minimums (fig. 4.5b) where antiresonant conditions for the even order modes are achieved. As opposite to standard ARROW-A waveguides, odd order modes do not have local minimum, but are directly transferred to asymmetrical modes of the LAS pair ($TE_{as,0}$), causing the coupling between the modes of the structures $d_{1,lat}$ to appear. As $h_{1,lat}$ decreases, the antiresonant regions changes in value, broadens, smoothers and slightly increases its attenuation. All the previously mentioned properties can be associated to minor confinement due to a weaker LAS.

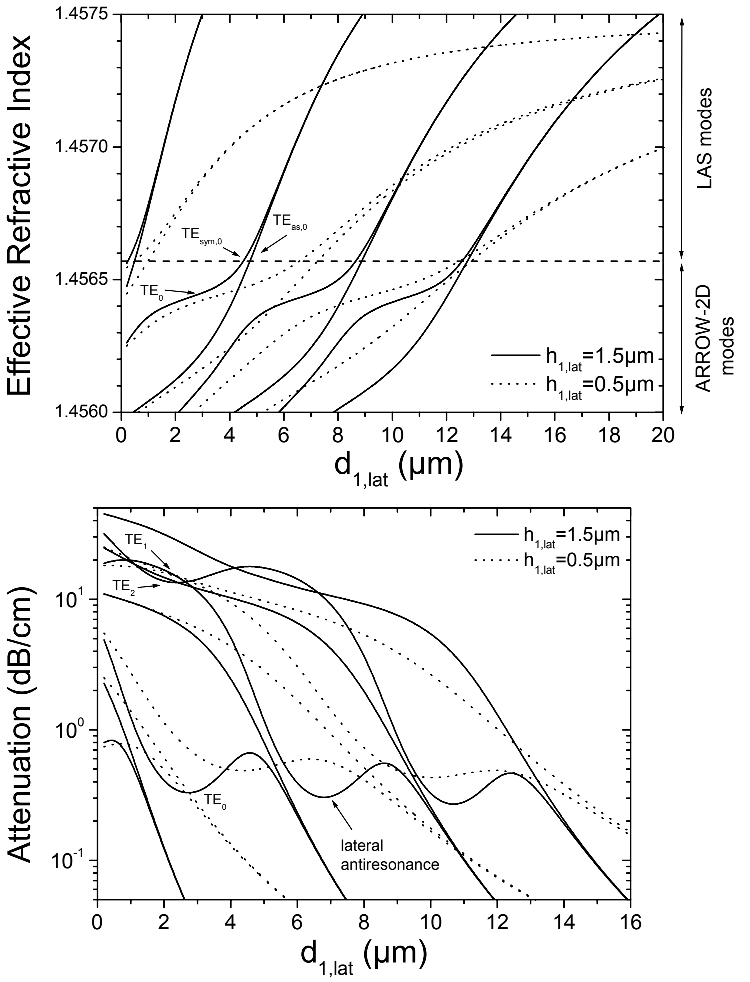

a)

b)

Fig 4.5. Dispersion (a) and attenuation (b) as a function of the width of the lateral antiresonant structure for two different heights $h_{1,lat}$ on a 15-µm width ARROW-2D waveguide.

A more intuitive approach can be done with the help of the field amplitude profiles shown in fig 4.6. and 4.7. They correspond to a 15μm-width ARROW-2D waveguide with $h_{1,lat}$=1.5μm and $d_{1,lat}$ at its first ($d_{1,lat}$=2.8μm) and second ($d_{1,lat}$=8.5μm) antiresonant condition, respectively. As can be seen, there only are three lateral modes in the whole structure if $d_{1,lat}$ is at its 1^{st} antiresonant condition (the second ARROW mode is shown by means of rigorousity, but its higher losses causes to be non-guided). These modes correspond to the symmetric (a) and asymmetric (b) modes of the directional coupler, together with the ARROW-2D mode (c). Things become more complex at the second antiresonant condition, since apart from the previously mentioned modes, there also exist coupling between the higher order modes of the directional coupler. Thus, if the LAS is chosen so as to work in the second antiresonant condition, one would expect up to 5 different modes, being the four first modes of the directional coupler and the last an ARROW mode. Although it is not a problem as far as guiding is concerned, it could present a drawback when measuring, since there would be more light propagating through non-desired zones that could cause an offset on the measures. Moreover, working at the second antiresonant condition does not provide with supplementary benefits as compared to first condition. Thus, it is desirable to work at this latter, only having then two directional coupler modes.

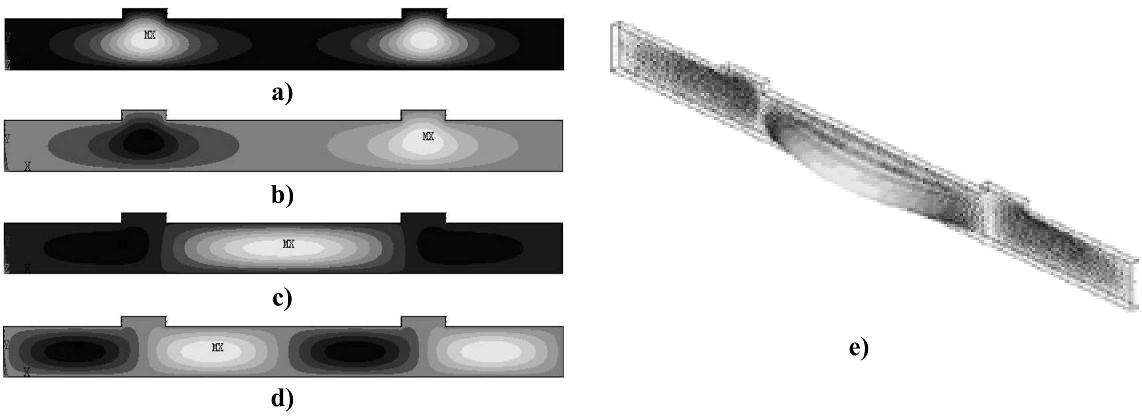

Fig 4.6. Modes in an ARROW-2D waveguide with d_c=3μm; d_1=0.35μm; d_2=d_c/2; $d_{c,lat}$=15μm; $d_{2,lat}$=$d_{c,lat}$/2, $h_{1,lat}$=0.5μm and $d_{1,lat}$=2.8μm (at its first antiresonant condition). a) TE_{sym}, b) TE_{ass}, c) TE_0 ARROW mode, d)TE_1 ARROW mode; e) vectorial plot of the TE_0 mode.

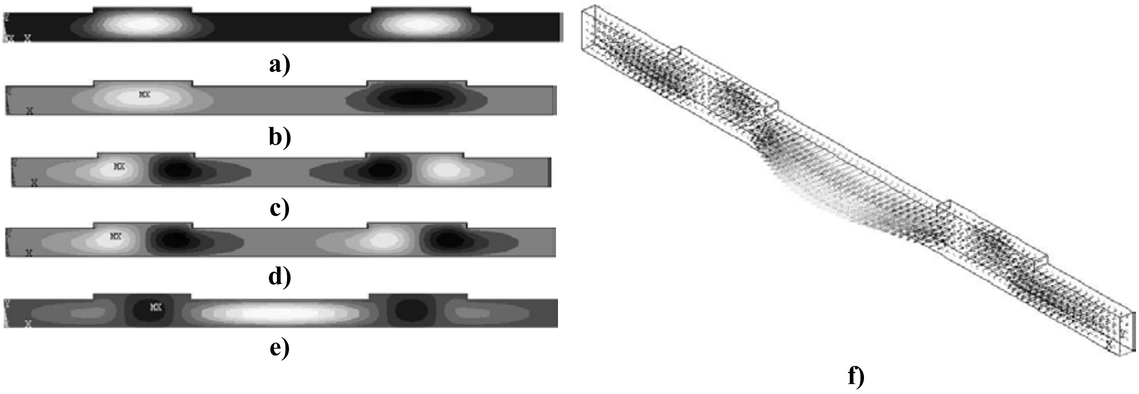

Fig 4.7. Modes in an ARROW-2D waveguide with d_c=3μm; d_1=0.35μm; d_2=d_c/2; $d_{c,lat}$=15μm; $d_{2,lat}$=$d_{c,lat}$/2, $h_{1,lat}$=0.5μm and $d_{1,lat}$=8.5μm (at its second antiresonant condition). a) $TE_{sym,0}$; b) $TE_{ass,0}$; c) $TE_{sym,1}$; d) $TE_{ass,1}$; e &f) TE_0 ARROW mode.

Finally, the fact that $d_{1,lat}$ is much wider in ARROW-2D as compared to slab-ARROW can again be explained by the small difference on the effective refractive index that it is achieved (only 1.6x10^{-3}) when comparing $h_{1,lat}$ from 0 to 1.5μm. Thus, the LAS obtained by this way is still weak and requires $d_{1,lat}$ with micron size. Although this in principle is a drawback, it has some advantages from the technological point of view, since it can be easily obtained by standard photolithographical processes (it has to be remembered that this technological step has a maximum resolution of 2μm and that, for $h_{1,lat}$=1.5μm, $d_{1,lat}$ should be 3μm). Moreover, since there is no limitation on the number of LAS located at both sides of the core, a better confinement can be achieved defining several LAS at both sides of the core. In fig. 4.8, the attenuation as a function of the lateral core thickness (a) and the lateral 1st cladding width (b) has been studied for an ARROW-2D waveguide with $h_{1,lat}$=1.5μm and double antiresonant pairs on each side of the core. Comparing the results obtained with figures 4.4 and 4.5, it can be seen that basically, the structure behaves in the same way as it did the simple ARROW-2D structure. The antiresonant regions, although they have not been displaced (which is logical, since neither the effective refractive indexes nor the core dimensions or the working wavelength of 633nm have been changed) nearly have an attenuation two orders of magnitude lower as compared to ARROW-2D with single LAS pair. Obviously, having two LAS on each side of the waveguide increases the light confinement, but it also increases the number of directional coupler modes, even if $d_{1,lat}$ is at its first antiresonant condition. The better overall confinement causes the structure to be multimode for $d_{c,lat}$ values above 20μm. In the same way of ARROW-2D, the ARROW mode is transferred to the symmetrical lowest order mode of the directional coupler. Neither the asymmetrical nor the higher order modes do play a significant role on the ARROW-2D structure with double LAS pairs.

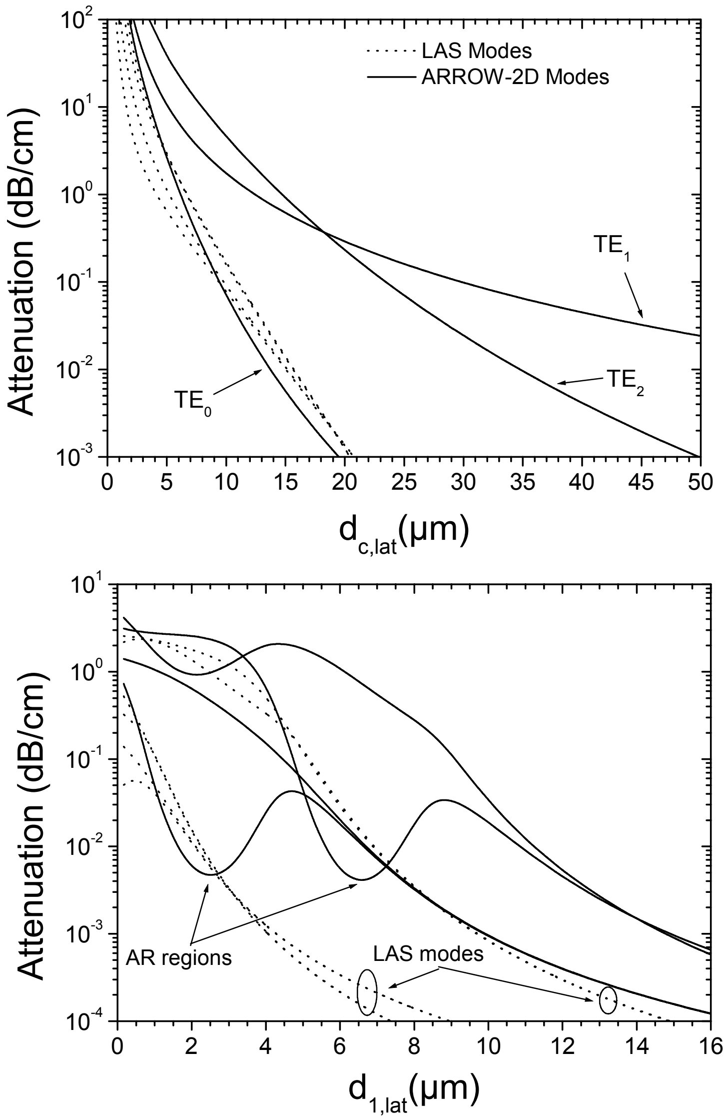

a)

b)

Fig 4.8. Attenuation as a function of the width of the lateral core (a) and of the lateral antiresonant structure (b), with $h_{1,lat}$=1.5μm on a 15-μm width ARROW-2D waveguide.

The different modal profiles for this latter structure shown in fig. 4.9a-d are due to fact that the double ARROW-2D waveguide has LAS whose modes can be coupled. As can be seen, all possible coupling combinations between $d_{1,lat}$ modes are obtained. ARROW mode (e & f) presents the expected enhancement of its confinement,